Mechanics of carbon nanotube scission under sonication

J. Stegen

Citation: The Journal of Chemical Physics **140**, 244908 (2014); doi: 10.1063/1.4884823
View online: http://dx.doi.org/10.1063/1.4884823
View Table of Contents: http://scitation.aip.org/content/aip/journal/jcp/140/24?ver=pdfcov
Published by the AIP Publishing

Mechanics of carbon nanotube scission under sonication

J. Stegen[a)]
Applied Physics, Eindhoven University of Technology, P.O. Box 513, 5600 MB Eindhoven, The Netherlands and Institute for Theoretical Physics, Utrecht University, Leuvenlaan 4, 3584 CE Utrecht, The Netherlands

(Received 13 March 2014; accepted 11 June 2014; published online 27 June 2014)

As-produced carbon nanotubes come in bundles that must be exfoliated for practical applications in nanocomposites. Sonication not only causes the exfoliation of nanotube bundles but also unwanted scission. An understanding of how precisely sonication induces the scission and exfoliation of nanotubes will help maximising the degree of exfoliation while minimising scission. We present a theoretical study of the mechanics of carbon nanotube scission under sonicaton, based on the accepted view that it is caused by strong gradients in the fluid velocity near a transiently collapsing bubble. We calculate the length-dependent scission rate by taking the actual movement of the nanotube during the collapse of a bubble into account, allowing for the prediction of the temporal evolution of the length distribution of the nanotubes. We show that the dependence of the scission rate on the sonication settings and the nanotube properties results in non-universal, experiment-dependent scission kinetics potentially explaining the variety in experimentally observed scission kinetics. The non-universality arises from the dependence of the maximum strain rate of the fluid experienced by a nanotube on its length. The maximum strain rate that a nanotube experiences increases with decreasing distance to the bubble. As short nanotubes are dragged along more easily by the fluid flow they experience a higher maximum strain rate than longer nanotubes. This dependence of the maximum strain rate on nanotube length affects the scaling of tensile strength with terminal length. We find that the terminal length scales with tensile strength to the power of 1/1.16 instead of with an exponent of 1/2 as found when nanotube motion is neglected. Finally, we show that the mechanism we propose responsible for scission can also explain the exfoliation of carbon nanotube bundles. © *2014 AIP Publishing LLC*. [http://dx.doi.org/10.1063/1.4884823]

I. INTRODUCTION

Carbon nanotube-based polymer composites[1–3] are promising new materials in which carbon nanotubes are, for example, used to create transparent conductive layers.[4,5] Dispersions of exfoliated nanotubes are required for the production of these so-called latex based nanotube composites.[1] Such dispersions can be obtained by means of sonication,[6–12] however, sonication also induces scission of nanotubes. Scission is unwanted because the quality of nanotube composites strongly depends on nanotube length.[13] Hence, the subject of nanotube scission under sonication has received some attention in literature.[14–24] There has however been little theoretical work on the scission mechanics of carbon nanotubes under sonication.[15,16,19,22,23] In fact, no attempt to describe exfoliation and scission simultaneously has been made. Such a description is highly relevant for it would, in principle, allow for the determination of optimal sonication settings. Pertinent questions that arise in this context include: How can a maximum degree of exfoliation and a minimum of nanotube scission under sonication be achieved? How can sonication be used to control the length distribution of a nanotube dispersion? This article provides a first step towards answering these questions.

During sonication an acoustic field is applied to a liquid and the resulting interaction between small bubbles in it and the acoustic field is known as acoustic cavitation.[25–31] In the process of acoustic cavitation, oscillations of the acoustic pressure cause the growth of microbubbles due to rectified diffusion.[31] These become unstable above a critical bubble radius.[28,30,32] The instability leads to the explosive growth of the bubble up to some maximum radius[32] and ends in the violent transient collapse of the bubble.[26] The violent nature of transient cavitation has been used to cut a wide variety of macromolecules, including carbon nanotubes. Much attention has been devoted to the disentanglement and scission of polymers.[33,34] The degradation of DNA[35] and the fragmentation of other fiber-like structures such as protein fibrils[36] has been studied. All of these macromolecules have a high aspect-ratio, which makes them sensitive to the strong gradients in fluid velocity that accompany the transient collapse of a bubble. The exact scission mechanism will however depend on the atomic structure of the macromolecule. Relevant in this regard is the work by Yu *et al.* who have studied the mechanics of scission under tension for single and multi-wall carbon nanotubes as well as that of single-wall nanotube ropes.[37,38] They observed that scission occurs in the outer tubes as, in their experiments, forces are primarily exerted on these tubes. We expect that similar scission mechanisms are at play during sonication. Here too, forces are primarily exerted on the outer tubes by the fluid flow, potentially leading to layer-by-layer scission of multi-wall nanotubes and to exfoliation of nanotube bundles.

a)Electronic mail: j.stegen@tue.nl

The mechanics of nanotube scission under sonication is determined by the interaction between the flow set up in the fluid following the transient collapse of a bubble and a nanotube. Following the model for polymer scission under sonication, as proposed by Kuijpers *et al.*,[33] Hennrich *et al.* attributed the scission of carbon nanotubes to the high strain rate of the fluid flow resulting from the transient collapse of the bubble. Strong viscous drag forces exerted by the fluid on the nanotube, which is radially aligned in the flow field, are responsible for scission of the nanotube. In particular, they demonstrated that the total drag force exerted by the fluid on the nanotube is proportional to the square of the nanotube length, and realised that this implies a terminal nanotube length below which scission can no longer occur.[15] This idea was reformulated by Ahir *et al.* in a simple model that gives a mathematical expression for the minimum nanotube length that can be reached by sonication for a given maximum strain rate experienced by the nanotube.[16] Lucas *et al.* realised that the scission rate of nanotubes should be length-dependent and is related to the probability that a nanotube is close to a cavitating bubble. Because a longer nanotube sweeps out a larger volume it is more likely to be close to a cavitating bubble and should thus break more easily. Their experimental results show a power law dependence of the average nanotube length on the amount of supplied acoustic energy.[19] A power law decay of the average length has been reported by other groups as well, albeit that the reported value of the exponent seems to be non-universal.[11,15,19,21] A very similar result was obtained for the *exfoliation* of nanotube bundles under sonication,[11,12] indeed suggesting that perhaps the same mechanism is responsible for scission and exfoliation.

Although the mechanism by which scission is thought to occur, that is, under tension, is well established, there has been some discussion on the role of buckling-mediated scission of nanotubes. Simulations by Chew *et al.* suggest that nanotubes enter the bubble during explosive growth and are expelled from the bubble due to their inertia in the final stages of collapse. After expulsion from the bubble into the liquid, the tangentially oriented nanotubes buckle and break due to overbending.[22] Pagani *et al.* argue that the mechanism proposed by Chew *et al.* is relevant only to a tiny fraction of carbon nanotubes for most nanotubes never get sufficiently close to the bubble to be absorbed into it.[23] Their simulations show that the scission mechanism is length-dependent, long nanotubes are expected to buckle and break while short nanotubes orient radially and break under tension, where the crossover-length between the two mechanisms is determined by the bending stiffness of the nanotube. Furthermore, they realised that there is a critical distance between bubble and nanotube at the start of bubble collapse beyond which no scission occurs: beyond this critical distance the fluid strain rate around the nanotube does not become sufficiently high. Finally, and importantly, Pagani *et al.* show that the two proposed mechanisms lead to different exponents for the power law describing the average nanotube length as a function of time, thus potentially explaining the non-uniformity of experimental results.[23]

Here we expand on earlier work[15,16,19,22,23] and primarily investigate the mechanics of nanotube scission under tension in detail, by taking nanotube motion during bubble collapse explicitly into account. In doing so, we find that the kinetics of scission under tension are non-universal, potentially providing an alternative to the mechanism proposed by Pagani *et al.*[23] as responsible for the variety in experimentally determined scission kinetics that are reported in literature. In our model, we approximate a carbon nanotube as a rigid, inexstensible rod. We characterise the process of transient cavitation by two length scales, being the typical bubble radius before and after explosive growth. We model the collapse of a bubble using the empty cavity approximation,[39] because, unlike the Rayleigh-Plesset equation[26] it gives a universal analytical relation between the bubble radius and the velocity of the bubble wall, which allows for the derivation of a universal equation giving the stress exerted on a nanotube by the fluid as a function of bubble radius. Furthermore, we make plausible that it is a reasonable approximation for the mathematically more complicated but more realistic Rayleigh-Plesset equation.[26] To describe the interaction between the fluid and the nanotube we invoke first-order slender-body theory,[40,41] and by assuming Stokesian dynamics, we derive the equations of motion for the temporal evolution of the translation and rotation of the nanotube. Using these equations of motion we investigate the scission mechanics for radially aligned nanotubes by taking the actual motion of nanotubes during bubble collapse explicitly into account.

By taking nanotube motion into account, we derive a length-dependent scission rate that is determined by the critical initial distance between nanotube and bubble below which scission occurs. We find that the scission rate depends on nanotube properties, such as their length and tensile strength, as well as on the sonication conditions. For nanotubes significantly longer than the terminal length, the scission rate scales with L^2, in agreement with earlier work.[15,23] However, when approaching the terminal nanotube length, deviations from this scaling law arise. This gives rise to non-universal scission kinetics, where the mean nanotube length scales as $t^{-\alpha}$ with $\alpha \leq 0.5$ a non-universal exponent. This is in agreement with experimental results where exponents varying between 0.22[19] and 0.5[15] have been reported, but contrasts with earlier work where scission of radially aligned nanotubes under tension was thought to result in universal scission kinetics.[15,16,18,19] We furthermore find that the minimum scission length, the nanotube length below which no scission can occur, scales as $\sigma_T^{1/1.16}$ when nanotube motion is taken into account instead of the previously predicted $\sigma_T^{1/2}$,[15,16,18,19] where σ_T is the tensile strength of the nanotube. The terminal length, the shortest nanotube segments that can be produced by sonication, follows an identical scaling relation with tensile strength for it is equal to approximately half the minimum scission length. Finally, we briefly discuss the implications of our model for the competition between scission under tension and buckling mediated scission as proposed by Pagani *et al.*[23] and we make plausible that the mechanism responsible for scission can provide an explanation for the exfoliation of carbon nanotube bundles.

The remainder of this article is organised as follows: in Sec. II we discuss the model that we invoke to describe a bubble undergoing transient cavitation. In Sec. III we present our

description of a nanotube and the interaction it has with a cavitating bubble. In Sec. IV we combine the models of Secs. II and III to determine the motion of and the forces exerted on a radially oriented nanotube during bubble collapse. Subsequently, in Sec. V we investigate the implications of the results from Sec. IV for scission kinetics. The article concludes with a discussion in Sec. VI, where we propose a scission-mediated exfoliation mechanism.

II. BUBBLE DYNAMICS

Any attempt to describe the mechanics of carbon nanotube scission under sonication requires three key ingredients: (1) a model describing fluid motion during transient cavitation, (2) a model for a carbon nanotube, and (3) a model for the interaction between the nanotube and the fluid. In this section we discuss the first ingredient and give a brief and simple overview of the process of transient cavitation. We discuss relevant length scales and show how the assumption of incompressibility in combination with Rayleigh's model for the collapse of an empty cavity[39] provides a full description of the fluid flow following the transient collapse of a bubble. It is explained why we use the empty cavity approximation rather than the more accurate and more frequently used Rayleigh-Plesset equation.[26] We shall be using the results of this section in Sec. IV, where we study the mechanics of scission under tension for radially aligned nanotubes. Before that, in Sec. III, we discuss our model of a nanotube and the interaction between a nanotube and a fluid flow.

During sonication an acoustic field is applied to a liquid, causing oscillations in the size of small bubbles present within the liquid. This is known as stable cavitation.[26,27] Due to rectified diffusion,[31] i.e., the net diffusion of dissolved gas into an oscillating bubble, these small bubbles slowly grow over many pressure cycles up to a critical radius, the so-called Blake threshold, for a discussion of which we refer to the literature.[28,30,32] This threshold is determined by the amplitude of the applied acoustic field and the surface tension of the bubble surface. It separates stable and transient cavitation, the latter being initiated when the surface tension can no longer contain the growth of the bubble during the negative pressure peak or the rarefaction phase of the applied acoustic field. The bubble then undergoes explosive growth and, assuming it grows sufficiently much, it undergoes transient collapse during the next positive pressure peak of the acoustic field.[32] The maximum bubble radius is reached when growth eventually slows down as the rarefaction phase ends and the acoustic pressure becomes positive.[32] Collapse of the bubble is now initiated by the still increasing acoustic pressure.[26] A schematic overview of the various stages of a bubble in an acoustic field is shown in Fig. 1. The bubble sizes as shown for the various stages are not drawn to scale.

To model transient cavitation, we consider a single spherical bubble within an incompressible liquid medium. To the liquid, a harmonic acoustic field, $p(t)$, with frequency ω and amplitude p_a is applied,

$$p(t) = -p_a \sin \omega t, \tag{1}$$

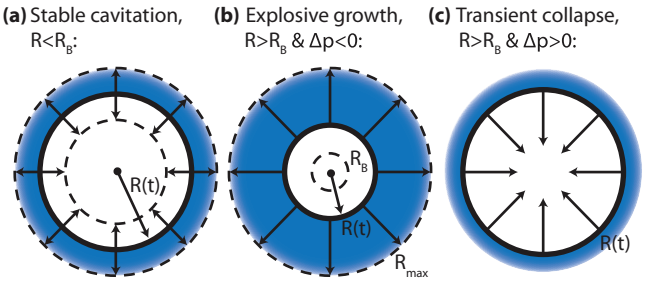

FIG. 1. Overview of bubble dynamics: (a) For bubbles with a radius $R(t)$ smaller than the Blake threshold, R_B, small amplitude oscillations in bubble radius, indicated schematically by double-pointed arrows, are induced by the acoustic field. The bubble slowly grows over many pressure cycles through rectified diffusion.[31] (b) The bubble radius exceeds the Blake threshold and grows explosively so long as the pressure within the fluid is smaller than that in the bubble, $\Delta p < 0$. At the end of explosive growth the bubble has a maximum radius, R_{max}, given by Eq. (3). (c) The pressure difference between fluid and bubble becomes positive, $\Delta p > 0$, and the bubble collapses violently as described by Eqs. (4) and (5). Note that the bubble sizes shown for the various stages are not to scale.

where $p_a = \sqrt{2P_{ac}\rho c/A_{son}}$ is the acoustic pressure amplitude with ρ the mass density and c the speed of sound in the liquid, while P_{ac} is the power of the applied acoustic field and A_{son} is a typical surface area through which the acoustic field passes. We approximate A_{son} by the surface area of the sonicator horn, which should be seen as a lower estimate for A_{son}. Using typical sonication conditions,[42] that is, a power of 40 W, a frequency of 20 kHz, and a sonicator horn of 15 mm diameter, we find a typical acoustic pressure amplitude of $p_a = 8.2 \times 10^5$ Pa for sonication in water under ambient conditions.

We can now turn to the following question: How does the size of a bubble prior to undergoing explosive growth compare to the mean size of a nanotube for a typical sonication experiment?[42] We find by calculation of the Blake threshold,[28,30,32] that bubbles with a radius larger than 0.1 μm grow explosively while at higher sonication power this radius is even smaller. Hence, in most practical situations the length of a nanotube, which we assume to be of the order of a micron, exceeds the radius of a bubble undergoing stable cavitation by at least a factor 5.

This leads us to the following question: how large is a bubble after it has reached the Blake threshold and undergone explosive growth? To answer this question, it seems reasonable to presume that growth of the bubble occurs when the pressure in the surrounding liquid is lowered by the applied acoustic field to a value below the pressure within the bubble. If we follow Apfel,[32] then the average bubble-wall velocity during this period must be $v_g = \sqrt{4(p_a - p_0)/9\rho}$, where $2(p_a - p_0)/3$ is the average pressure difference between the interior of the bubble and the surrounding liquid during this period and p_0 is the ambient pressure in the liquid in the absence of an applied acoustic field. This average velocity follows from Rayleigh's model for the collapse of an empty cavity which we will discuss shortly.[39] If we multiply this average velocity with the time that the interior bubble pressure, which we assume to be zero, exceeds the pressure in the surrounding liquid, that is, the time for which $p(t) + p_0 < 0$ where $p(t)$ is

given by Eq. (1), we obtain a first approximation for the maximum bubble radius. The time for which $p(t) + p_0 < 0$ holds is approximately equal to $t_g = 2\sqrt{2(1 - p_0/p_a)}/\omega$.[32] If we multiply this period of time with the average velocity of the bubble wall during this period, we obtain a first approximation for the maximum bubble radius,

$$R_1 = \frac{4}{3\omega}(p_a - p_0)\sqrt{\frac{2}{p_a\rho}}. \tag{2}$$

Note that we neglected the radius the bubble has prior to undergoing explosive growth and assume R_1 to be equal to the amount by which the bubble radius increases. This is reasonable because the bubble radius typically grows by several orders of magnitude during explosive growth.

This approximation may be improved upon by taking into account that the bubble remains to grow even after the pressure in the surrounding liquid exceeds the pressure in the bubble. In this period the accumulated kinetic energy of the fluid flow is dissipated as pressure-volume work. By accounting for this Apfel obtained the following equation for the maximum bubble radius after explosive growth,[32]

$$R_{max} = \frac{4}{3\omega}(p_a - p_0)\sqrt{\frac{2}{p_a\rho}}\left[1 + \frac{2(p_a - p_0)}{3p_0}\right]^{1/3}, \tag{3}$$

where the last factor of the equation is the correction to our first approximation. Equation (3) allows us to estimate the maximum bubble radius after explosive growth for a typical sonication experiment,[42] which turns out to be of the order of 0.7 mm. The actual maximum bubble radius is somewhat smaller than this, because viscous effects were neglected in the derivation of Eq. (3). Interestingly, this implies that the correction factor included in Eq. (3), which is typically of the order of unity, is not necessarily an improvement on Eq. (2). Nonetheless, bubbles are, at the end of explosive growth, typically at least a factor 100 or more larger than the typical length of a carbon nanotube, which we again assume to be of the order of a μm.

After the bubble has reached a maximum radius, the acoustic pressure is positive and the final stage of transient cavitation is initiated, being the violent collapse of the bubble. It is during this stage of transient cavitation that nanotube scission occurs as the fluid flow subjects the nanotube to a high stress. We are interested in obtaining an expression for the fluid velocity as a function of time and distance from the center of the collapsing bubble. The radial dependence of the fluid velocity is fully determined if the bubble is assumed to remain spherical at all times and if the fluid is assumed to be incompressible. We presume both these assumptions to hold. Let the bubble radius be denoted as $R = R(t)$, the velocity of the bubble wall as $\dot{R} = \dot{R}(t)$ and the fluid velocity at a distance r from the center of the bubble as $\vec{v}(r, t)$. The radial dependence of the fluid velocity as a function of the radius of the bubble and the velocity of the bubble wall is then,

$$\vec{v}(r, t) = \frac{R^2(t)\,\dot{R}(t)}{r^2}\hat{e}_r, \tag{4}$$

where $\hat{e}_r$ is the radial unit vector.

Equation (4) requires as input a model for the bubble radius as function of time. Even though the Rayleigh-Plesset equation[26] is a better and more frequently used model, we use the empty cavity approximation as proposed by Rayleigh[39] to model this, for it leads to a universal and mathematically tractable description of transient cavitation, which is easily applied. As we will see in Secs. IV and V, it allows us to quantify the interaction between a nanotube and a collapsing bubble in terms of a few dimensionless numbers. Rayleigh derived the empty cavity approximation by modeling the bubble as an empty cavity that is filled up by fluid during its collapse, and by assuming that the energy released by pressure-volume work during collapse is converted into the kinetic energy of the fluid moving in to fill the cavity. This allowed him to derive a simple equation describing the transient collapse of a bubble. It takes the following dimensionless form:

$$\frac{dx}{d\tau} = -\sqrt{\frac{1 - x^3}{x^3}}, \tag{5}$$

where $x = R(t)/R_{max}$ is the dimensionless bubble radius and $\tau = t/t_c$ the dimensionless time with $t_c = \sqrt{3\rho {R_{max}}^2/2p}$ a measure for the lifetime of the collapsing bubble, p is the (static) pressure difference between the inside and outside of the bubble and ρ is, as before, the fluid mass density. In the derivation of Eq. (5) a static pressure difference between the bubble and the surrounding liquid, p, is assumed, in reality it is not static and the value of p must be approximated. We approximate p by the sum of the ambient pressure and the root-mean-square acoustic pressure, $p = p_a/\sqrt{2} + p_0$. For given sonication conditions, Eqs. (3)–(5) fully describe the fluid flow during the collapse of a bubble.

The question arises whether the description of transient cavitation as given by these equations is a good description. How do the results from Eqs. (3)–(5) compare to results of the more advanced Rayleigh-Plesset equation?[26] This equation is not reproduced here, but unlike Eq. (5) it does include inertial and viscous effects as well as a time-dependent acoustic pressure. This question is in part answered by Fig. 2, which shows the bubble radius and fluid strain rate at the surface of the bubble as a function of time during bubble collapse for a

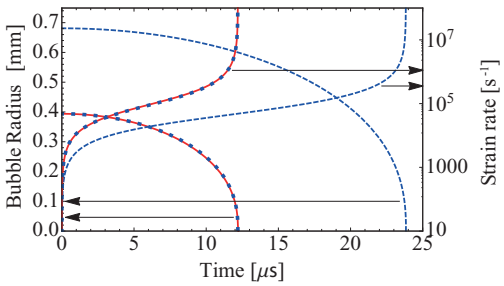

FIG. 2. The bubble radius and strain rate at the bubble surface, $\dot{\epsilon} = \dot{R}(t)/R(t)$, as a function of time during the transient collapse of a bubble for a typical sonication experiment.[42] Dashed blue lines represent the solution as obtained from the empty cavity approximation while the solid red line represents the solution obtained from the Rayleigh-Plesset equation. The solution of the empty cavity approximation, with length and time scales matched to the solution of the Rayleigh-Plesset equation, is represented by the dotted blue line. Note that it is virtually identical to the solution of the Rayleigh-Plesset equation.

typical sonication experiment[42] as determined by the empty cavity approximation (dashed blue line), the Rayleigh-Plesset equation (solid red line) as well as for the empty cavity approximation with length and time scales matched to the solution of the Rayleigh-Plesset equation (dotted blue line). The solution of the empty cavity approximation was obtained by numerically solving Eq. (5) where R_{max} is determined by Eq. (3) and the average pressure difference between bubble and the surrounding liquid, p, is approximated as $p_a/\sqrt{2} + p_0$. The Rayleigh-Plesset equation was solved for a full acoustic cycle, as given by Eq. (1), using the methodology of Pagani *et al.*,[23] and by using an initial bubble radius of 0.1 μm, which equals the Blake radius for the given sonication conditions, only the collapse phase is shown here. From Fig. 2 it is clear that solutions of the empty cavity approximation (dashed blue line) and the Rayleigh-Plesset equation (solid red line) do not match quantitatively even though the shapes of the curves are virtually identical. This is not so much the result of the poor quality of the empty cavity approximation but rather a result of a poor choice for the corresponding length and time scale, R_{max} and t_c.

How good is the empty cavity approximation if we rescale it to have it match time and length scales with the results from the Rayleigh-Plesset equation? In this case the agreement is excellent, the solutions of the rescaled empty cavity approximation (dotted blue line) and the Rayleigh-Plesset equation (solid red line) are virtually identical. For typical sonication settings,[42] the relative error in bubble radius and strain rate as given by the rescaled empty cavity approximation and as compared to the solution obtained from the Rayleigh-Plesset equation is less than 4% at all times. In an identical manner we compared the solution of the Rayleigh-Plesset equation and the rescaled empty cavity approximation for all combinations of acoustic powers of $P_{ac} = 10$ W, 40 W, and 160 W, acoustic frequencies of 10, 20, and 40 kHz and initial bubble radii of 0.1 R_B, 1 R_B, and 10 R_B. In doing so, we find the following, when a bubble has an initial radius of 0.1 R_B it undergoes stable cavitation as surface tension prevents the explosive growth of the bubble. For bubbles with an initial size of 1 R_B and 10 R_B we observe transient cavitation, in agreement with the definition of the Blake threshold. Here, we observe that the quality of the rescaled empty cavity approximation decreases with increasing acoustic power and increasing initial bubble radius, the relative error in bubble radius and strain rate reaches a maximum of approximately 35% and 45%, respectively, for an acoustic power of 160 W and an initial bubble radius of 10 R_B, while its quality appears to be independent of the acoustic frequency.

Note that even for a maximum relative error of 35% in the bubble radius and 45% in the strain rate, the disagreement is only quantitative. By matching the length and time scales of the empty cavity approximation to the solution of the Rayleigh-Plesset equation we assure that begin and end points of both curves are identical. Furthermore, an expansion of both the Rayleigh-Plesset equation and the empty cavity approximation yield identical behaviour for the initial stages of bubble collapse.[43] In conclusion, the empty cavity approximation is typically very good but our approximation of the associated typical length and time scale of the transient collapse is poor. Fortunately, we can improve upon this poor approximation by determining the correct length and time scales directly from the solution of the Rayleigh-Plesset equation and use these values as input for the rescaled empty cavity approximation. Note that in the derivation of both the Rayleigh-Plesset equation and Rayleigh's model for the collapse of an empty cavity the fluid is presumed to be incompressible. As it is the assumption of incompressibility that leads to the strong gradient in the fluid velocity, which is responsible for nanotube scission, we feel confident in using Rayleigh's model for the collapse of an empty cavity because it captures the essential physics of the process.

Having described the process of transient cavitation, we can now investigate the interaction between a nanotube and the fluid flow generated by a bubble undergoing transient cavitation.

III. FLUID-NANOTUBE INTERACTION

The motion of, and the forces exerted on a carbon nanotube near a transiently cavitating bubble are determined by the interaction between that nanotube and the fluid flow following the transiently cavitating bubble. We focus attention on defect-free carbon nanotubes with lengths well below their persistence length, determined to be in excess of 26 μm,[44,45] and model them as rigid rod-like particles with diameter d, length L, and uniform tensile strength σ_T. Hence, in treating the nanotubes as rigid rod-like particles, we neglect any elastic bending and stretching of the nanotubes due to thermal fluctuations or the fluid flow. This is a reasonable approximation when studying the scission of radially aligned nanotubes under tension, because any bending of the nanotube is suppressed by the fluid flow. However, it does fail in the initial stages of bubble collapse, when a nanotube relaxes from a tangential orientation into either a stretched radially aligned or a highly bent conformation that can potentially lead to subsequent scission under tension or buckling-mediated scission respectively.[23] We return to this issue in Sec. VI.

By modeling the carbon nanotube as a rigid rod-like particle we are able to invoke first-order slender-body theory to model the viscous drag forces exerted on the nanotube by the fluid flow, just as in previous work on nanotube scission under sonication.[15,18,19,23] Slender-body theory[40,41] describes the viscous drag forces exerted on an elongated particle in a Stokes flow. Stokes flows are characterized by a small Reynolds number, $\mathrm{Re} \ll 1$,[46] implying that viscous effects are dominant over inertial effects. In our case, the Reynolds number is for most of the time typically small if we assume the typical length scale of interaction between the fluid flow and a nanotube to be the nanotube diameter. Intuitively this choice of length scale makes sense, because the fluid flow is "perturbed" by the radially aligned nanotube over a length equal to its diameter. However, in the final stages of collapse of the bubble the relative fluid velocity at the tips of the nanotube becomes very large. Indeed, a simple scaling analysis shows that the Reynolds number must reach a maximum of the order of unity near the nanotube tips at the moment of scission[47] but is smaller than that in the central part of the nanotube and prior to the moment of scission. Even though the assumption

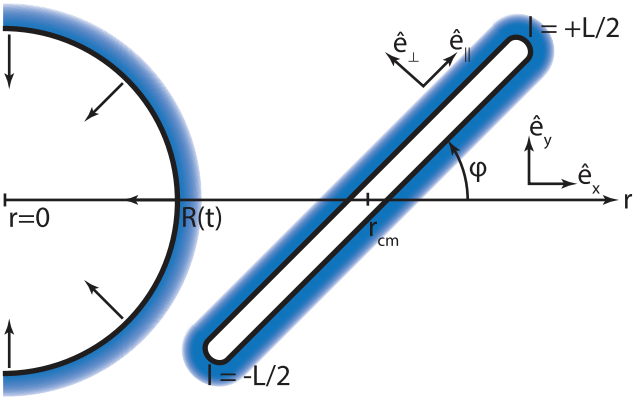

FIG. 3. The spatial geometry of the nanotube bubble interaction. The bubble has radius $R(t)$, the center of the nanotube of length L is at a distance r_{cm} from the center of the bubble and at an angle φ from a radial orientation. The contour distance away from the center of mass of the nanotube is given by l. Two coordinate systems are shown: $\hat{e}_x, \hat{e}_y$ denote, respectively, the direction perpendicular and the direction tangential to the bubble surface. Coordinate system $\hat{e}_\perp, \hat{e}_\parallel$ defines the directions parallel and perpendicular to the main axis of the nanotube.

of small Reynolds numbers does not quite hold at all times, it does hold for the majority of time and justifies our use of slender-body theory to model the fluid-nanotube interaction.

Before applying slender-body theory, we need to consider the geometry of the interaction between the bubble and the nanotube. Due to the presumed radial symmetry of bubble collapse and because the nanotube and the center of the bubble are always in a single plane, the fluid-nanotube interaction is reduced to a two-dimensional problem. The corresponding geometry is shown in Fig. 3, where $\hat{e}_x$ is the direction perpendicular to the bubble surface while $\hat{e}_y$ is a direction tangential to the bubble surface. Although rotational motion of the nanotube around $\hat{e}_x$ and out of the x–y plane is possible, we need not explicitly consider it. The reason is that the radial distance between any segment of the nanotube and the center of the bubble is invariant under any such rotation, that is, the geometry of the problem does not change as a result of this rotational motion. Furthermore, rotation around $\hat{e}_x$ affects neither translational nor rotational motion in the x–y plane, as we show below.

Within first-order slender-body theory,[40,41] the viscous drag force per unit length exerted by the fluid flow on the nanotube, $\vec{f}$, can be decomposed into a component parallel, $f_\parallel$, and perpendicular, $f_\perp$, to the main axis of the nanotube,

$$f_\parallel = 2\pi\mu v_{\parallel,rel}, \qquad f_\perp = 4\pi\mu\, v_{\perp,rel}, \tag{6}$$

where μ is the dynamic viscosity of the liquid, $v_{\parallel,rel}$ is the relative fluid velocity parallel to the axis of the nanotube, while $v_{\perp,rel}$ is the relative fluid velocity perpendicular to the axis of the nanotube. These velocities are relative ones, that is, relative to the translational and rotational motion of the nanotube. Here we neglect a logarithmic dependence of these forces on the aspect ratio of the nanotube, which is of the order of unity for experimentally relevant nanotube lengths.[15] The relative fluid velocity is given by,

$$\vec{v}_{rel} = \vec{v}\,(r) - \vec{v}_{cnt} - \dot{\varphi} l \hat{e}_\perp, \tag{7}$$

where $\vec{v}(r)$ is the local fluid velocity at a radial distance r from the center of the bubble as given by Eqs. (4) and (5), $\vec{v}_{cnt}$ is the translational velocity of the nanotube, $\dot{\varphi}$ denotes the angular velocity of the nanotube around its center of mass, l is the contour distance away from the center of mass of the nanotube, and $\hat{e}_\perp$ is a unit vector perpendicular to the main axis of the nanotube, all as shown in Fig. 3.

As mentioned, the fluid flow along the nanotube is presumed to be characterised by a small Reynolds number. For small Reynolds numbers, viscous effects predominate over inertial effects, implying an overdamped limit. Inertialess motion implies mechanical equilibrium, so the total force, $\sum \vec{F}$, and torque, $\sum \vec{\tau}$, exerted by the fluid on the nanotube must equal zero. The assumption of mechanical equilibrium leads to a set of equations of motion that are independent of the actual fluid viscosity and do allow for acceleration of the nanotube. Because this is a somewhat counter-intuitive result, two remarks are in order. First, acceleration is possible even if the total force and torque exerted on the nanotube by the fluid is assumed to be zero at all times, because the fluid-nanotube interaction is in the overdamped limit and inertial effects relax fast relative to the relevant timescale of nanotube motion. Second, the equations of motion are independent of fluid viscosity because the total force and torque exerted on the nanotube must equal zero and only forces of a viscous origin, Eq. (6), are exerted on the nanotube and these are all proportional to fluid viscosity.

Given a local fluid velocity, $\vec{v}(l)$, along the nanotube, where $l \in [-L/2, +L/2]$ denotes the contour distance away from its center, mechanical equilibrium implies zero net force,

$$\sum \vec{F} = \int_{-L/2}^{+L/2} \vec{f}\,(l)\, dl = 0, \tag{8}$$

and zero net torque,

$$\sum \vec{\tau} = \int_{-L/2}^{+L/2} l\hat{e}_\parallel \times \vec{f}\,(l)\, dl = 0, \tag{9}$$

where $\hat{e}_\parallel$ is a unit vector along the axis of the nanotube. Substitution of Eqs. (6) and (7) into Eqs. (8) and (9) yields the equations of motion for the nanotube,

$$\vec{v}_{cnt} = \frac{1}{L} \int_{-L/2}^{+L/2} \vec{v}\,(l)\, dl \tag{10}$$

and

$$\dot{\varphi} = \frac{12}{L^3} \int_{-L/2}^{+L/2} l v_\perp (l)\, dl, \tag{11}$$

where $v_\perp(l)$ is the component of the local fluid velocity which is perpendicular to the main axis of the nanotube (see Fig. 3). Note that the equations of motion, Eqs. (10) and (11), for a rod-like particle in a Stokes flow have been derived previously.[41] These equations of motion are instantaneously decoupled, that is, the instantaneous rotational velocity, $\dot{\varphi}$, and translational velocity, $\vec{v}_{cnt}$, are independent of each other as is

evident from Eqs. (10) and (11). This is so because rotational motion around the center of mass of the nanotube produces a local drag force proportional to $-\dot{\varphi} l$ of which the integral along the nanotube is always zero, while the net torque resulting from any translational motion is always zero for the local torque due to translational motion is again anti-symmetric in l. Note that this decoupling only holds instantaneously, translational motion does depend on the orientation of the nanotube and rotational motion depends on the position of the nanotube.

Above we reduced the interaction between a nanotube and a bubble to a two-dimensional problem. We claimed to be able to do this because translational and rotational motion within the plane spanned by the nanotube and the center of the bubble, i.e., the x–y plane as defined in Fig. 3, is independent of any rotational motion out of the x–y plane. We are now able to understand this. Indeed, the net drag force resulting from any rotational motion is zero and does not affect translational motion. Rotational motion in the x–y plane, as given by $\dot{\varphi}$, is not affected by rotational motion out of this plane for the torque resulting from such motion is perpendicular to the torque responsible for rotational motion in the x–y plane.

With the equations of motion as given by Eqs. (10) and (11) combined with Eqs. (4) and (5), which describe the fluid flow during bubble collapse, we are able to investigate the interaction between a nanotube and the fluid flow during various stages of transient cavitation. In Sec. IV we evaluate the motion of and forces exerted on a radially aligned nanotube during the transient collapse of a bubble.

IV. MECHANICS FOR A RADIALLY ALIGNED NANOTUBE DURING BUBBLE COLLAPSE

Let us assume that the nanotube has a fully stretched and perfect radial conformation throughout the process of bubble collapse, with angle $\varphi = 0$ as Fig. 3. In assuming this, we neglect the relaxation of a nanotube from an unstable tangential orientation, $\varphi = \pi/2$ in Fig. 3, in the initial stages of bubble collapse, which has been shown to occur by Pagani *et al.*[23] We return to this assumption and discuss the initial relaxation from a tangential orientation briefly in Sec. VI.

Let the nanotube have length L and let its tip closest to the bubble be at an initial distance r_0 from the center of a bubble with radius R_{max} that has just undergone explosive growth and is about to collapse. During bubble collapse the nanotube will be dragged along by the fluid and the distance between the center of the bubble and the nanotube will decrease. We denote the distance between the tip of nanotube closest to the bubble and the center of the bubble as $r_{cnt}(t)$ where $r_{cnt}(t = 0) = r_0$ (see Fig. 4).

Assuming incompressibility of the fluid and a spherically symmetric fluid flow, implicit in Eq. (4), and substituting $\vec{r}(l) = (r_{cnt} + L/2 + l)\hat{e}_x$, we can calculate the velocity of the nanotube straightforwardly from Eq. (10) to give,

$$\vec{v}_{cnt} = \frac{R^2 \dot{R}}{r_{cnt}\,(r_{cnt} + L)} \hat{e}_x, \tag{12}$$

where we note that R, $\dot{R}$, r_{cnt}, and v_{cnt} are functions of time and that v_{cnt} is the time derivative of the tip position, r_{cnt}, so

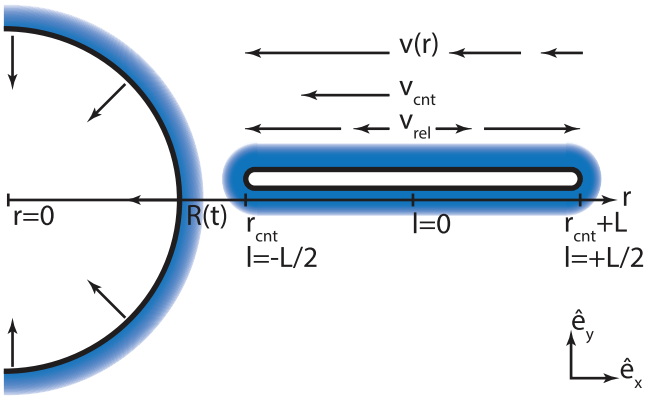

FIG. 4. The geometry of the interaction between a radially oriented nanotube and the fluid flow following the transient collapse of a bubble with radius $R(t)$. The distance between the tip of the nanotube, of length L, closest to the bubble and the center of the bubble is denoted by $r_{cnt}(t)$. The directions as given by $\hat{e}_x$ and $\hat{e}_y$ and the parameter l are as defined in Fig. 3. Above the nanotube the direction and magnitude of the actual fluid velocity $v(r)$, Eqs. (4) and (5), the nanotube velocity, Eq. (12), and the relative fluid velocity along the nanotube, Eq. (7), are shown.

$v_{cnt} = \dot{r}_{cnt}$. Integrating Eq. (12) over time by separation of variables, gives the nanotube position as a function of time. After rescaling all distances to R_{max}, as given by Eq. (3) or as obtained from a numerical solution of the full Raleigh-Plesset equation, see our earlier discussion in Sec. II, the dimensionless nanotube position $y(t) \equiv r_{cnt}(t)/R_{max}$ obeys,

$$y^3 - y_0^3 + \frac{3}{2}\tilde{L}\left(y^2 - y_0^2\right) = x^3 - x_0^3, \tag{13}$$

where $x = R(t)/R_{max}$ is the dimensionless bubble radius that we calculate from Eq. (5), $x_0 = 1$ for it is the value of x at the start of bubble collapse, $y_0 = r_0/R_{max}$ is the dimensionless distance between the center of the bubble and the tip of the nanotube closest to the bubble at the start of bubble collapse and $\tilde{L} = L/R_{max}$ is the dimensionless nanotube length.

By way of illustration we have plotted in Fig. 5 the motion of nanotubes of length $\tilde{L} = 0.05$ (dashed line, red) and $\tilde{L} = 0.2$ (dotted-dashed line, green) for two different initial distances $y_0 = 1$ and $y_0 = 1.15$ as obtained from Eq. (13). The values used for $\tilde{L}$ are unrealistically large but serve to

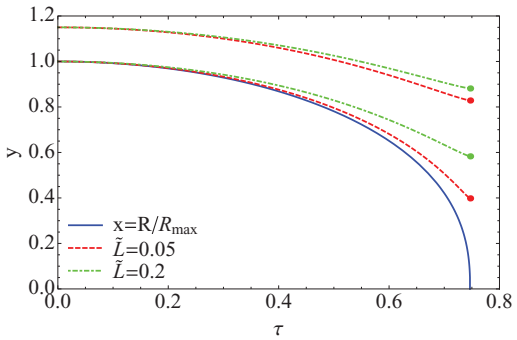

FIG. 5. The position of the tip of a nanotube scaled to R_{max} as a function of dimensionless time, τ, during bubble collapse. The dimensionless bubble radius x, Eq. (5), is indicated by the solid blue line. Nanotube motion as given by Eq. (13) is shown for $\tilde{L} = 0.05$ (dashed line, red) and $\tilde{L} = 0.2$ (dotted-dashed line, green) for an initial distance of $y_0 = 1$ and $y_0 = 1.15$.

highlight the dependence of nanotube motion on length and initial position. The dimensionless bubble radius, given by Eq. (5), is depicted by the solid blue line. Note that for $\tilde{L} \to 0$ and $y_0 = 1$ the motion of nanotube equals the motion of the bubble wall. From Fig. 5 it is clear that nanotubes cannot keep up with the wall of the collapsing bubble and that the nanotubes slow down as their length and/or initial distance from the bubble increases. This is easily understood from Eq. (10) that equates the nanotube velocity to the average of the local fluid velocity along the nanotube. Because the local fluid velocity decreases with distance as r^{-2}, nanotubes become slower with increasing initial distance from the bubble *and* with increasing length.

Having established where the nanotube is relative to the bubble from the moment it starts to collapse, we are now able to evaluate the maximum stress it is subjected to by the surrounding fluid as it is dragged along by the fluid during the collapse of the bubble. During bubble collapse the nanotube's velocity equals the average local fluid velocity along the nanotube because this ensures that the net force exerted on the nanotube equals zero. This is precisely the requirement of mechanical equilibrium that we used to derive the translational equation of motion, Eqs. (10) and (13). Although the net drag force experienced by the nanotube vanishes, viscous friction does exert a large stress on the nanotube. The *relative* fluid velocity along the part of the nanotube closest to the bubble is directed radially inward while that furthest away is directed outward (see Fig. 4). The stress exerted by the fluid is at a maximum at the point on the nanotube where the local fluid velocity, Eq. (4), is equal to the nanotube velocity, Eq. (12), and the relative fluid velocity is zero. Equating Eqs. (4) and (12), we find that the relative fluid velocity is zero and the stress on the nanotube maximal at a distance $r^*(t)$ from the center of the bubble,

$$r^*(t) = \sqrt{r_{cnt}(t)\,(r_{cnt}(t) + L)}. \tag{14}$$

Note that r^* is time-dependent as we are following the nanotube as it is dragged along by the fluid flow following the collapsing bubble. In Sec. V we show that r^* corresponds to a point on the nanotube that is close to center of mass of the nanotube.

The maximum stress on the nanotube, i.e., that at r^*, where the relative fluid velocity equals zero, is given by the difference of the forces exerted by the fluid on the segment of the nanotube where the relative fluid velocity is directed radially inward and the segment where it is directed radially outward, divided by A, the cross sectional area of the nanotube. The force exerted on each of these two segments is equal in magnitude but opposite in direction, again, ensuring that the nanotube remains in mechanical equilibrium. The magnitude of this force is then given by the absolute value of the integral of Eq. (6) along one of these two segments, where $\vec{v}_{rel}$ is given by Eqs. (7) and (12). In dimensionless form we find for the maximum stress on the nanotube at r^*,

$$\tilde{\sigma}_* = \sqrt{x - x^4}\left(\frac{1}{\sqrt{y}} - \frac{1}{\sqrt{y + \tilde{L}}}\right)^2, \tag{15}$$

where $\tilde{\sigma}_* = \sigma_*/\sigma_0$ is the dimensionless stress with σ_0 the characteristic stress scale as determined by experimental settings,

$$\sigma_0 = \frac{4\pi\mu R_{max}}{A}\sqrt{\frac{2p}{3\rho}}, \tag{16}$$

where μ is the dynamic viscosity of the liquid, R_{max} is the bubble radius just before the start of the collapse of the bubble, A is the cross sectional area of the nanotube, p is the (static) pressure difference between the interior of the bubble and the surrounding liquid, and ρ is the mass density of the liquid. Both y and $\tilde{\sigma}_*$ are functions of x, $\tilde{L}$, and y_0, so time enters implicitly. However, unlike Eq. (13), which is independent of the time-dependence of $x(t)$, Eq. (15) only holds for $x(t)$ as calculated from Rayleigh's model for the collapse of an empty cavity, Eq. (5). Note that Eq. (14) was derived previously by Ahir *et al.*,[16] who also derived an equation for the maximum stress on the nanotube. Their expression for the maximum stress exerted on the nanotube differs from our Eq. (15) because we explicitly model the fluid velocity using Rayleigh's model for the collapse of an empty cavity and explicitly take nanotube motion into account through Eq. (13).

Given the values of $\tilde{L}$ and y_0, nanotube motion is given as a function of x by Eq. (13). Substitution of this into Eq. (15) yields the stress at $r^*(t)$ as a function of $x(t)$. At some value of x the stress at r^* will be at a maximum, denote this value as $x = x_{max}$. Substitution of x_{max} into Eq. (15) yields the maximum stress, $\tilde{\sigma}_*^{max}$, experienced by the nanotube during bubble collapse as a function of its dimensionless length and initial distance to the center of the bubble,

$$\tilde{\sigma}_*^{max}(\tilde{L}, y_0) = \max[\tilde{\sigma}_*(x; \tilde{L}, y_0), 0 < x < 1]. \tag{17}$$

We have not been able to obtain an analytic expression for $\tilde{\sigma}_*^{max}$, so we determine it numerically. In Fig. 6, $\tilde{\sigma}_*^{max}$ is shown as a function of $\tilde{L}$ and y_0, the relation between the three parameters contains important information regarding the scission mechanics. A line over the surface at $y_0 = 1$ gives the dimensionless minimum nanotube length for which scission can occur as a function of dimensionless tensile strength, while lines at constant $\tilde{\sigma}_*^{max}$ give the dimensionless maximum initial distance between the nanotube and the bubble for which scission can occur as a function of dimensionless nanotube

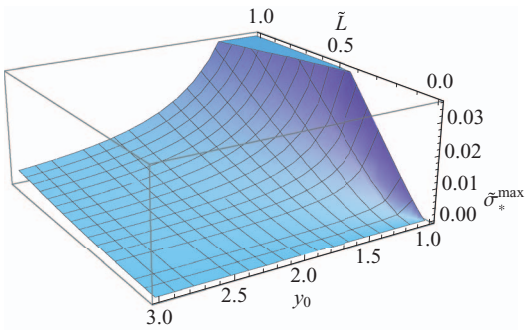

FIG. 6. The maximum dimensionless stress exerted on a nanotube during bubble collapse, $\tilde{\sigma}_*^{max}$, as a function of the dimensionless nanotube length, $\tilde{L}$, and the dimensionless distance, y_0, between the nanotube and the center of the bubble at the time of the start of the bubble collapse.

length. The scission rate is related to this maximum initial distance.

In summary, we have shown that the motion of a stretched and radially aligned nanotube during bubble collapse is determined by its length and initial distance away from the center of the bubble. As the fluid strain rate around the nanotube depends on the nanotube's position, the maximum stress experienced by a nanotube is determined by, again, its length and initial position as well as the sonication conditions through the characteristic stress scale σ_0. In Sec. V. we show how the minimum scission length and the scission rate can be determined from Fig. 6.

V. IMPLICATIONS FOR SCISSION KINETICS

In Sec. IV the motion of a radially oriented nanotube and the forces exerted on it during bubble collapse were calculated. The analysis resulted in Fig. 6, which gives the maximum stress exerted on the nanotube as a function of its length and of its initial distance away from the center of the bubble at the time of the start of the bubble collapse. From this figure it is clear that the maximum stress experienced by a nanotube increases with decreasing initial distance to the center of the bubble.

A nanotube of a given length then experiences a maximum stress when it starts out as close as possible to the surface of the bubble. The smallest initial distance between nanotube and bubble center allowed for in the model is $y_0 = 1$. Given $\tilde{L}$, the maximum dimensionless tensile strength, $\tilde{\sigma}_T$, of a nanotube of that length that will still break under sonication is given by $\tilde{\sigma}_T = \tilde{\sigma}_*^{max}(\tilde{L}, y_0 = 1)$, of which the value can be obtained by numerically solving Eq. (17). The shortest nanotube segments produced by sonication, the so-called terminal length, then depends on sonication conditions and the tensile strength of the nanotube. As we show below, scission occurs very close to the center of the nanotube, so the dimensionless terminal length is in good approximation equal to $\tilde{L}_{min}/2$, where $\tilde{L}_{min}$ is the dimensionless minimum scission length. The relation between the minimum scission length and tensile strength, as numerically determined from Eq. (17), can be fitted to a power law. The resulting power law in dimensionless form is,

$$\tilde{L}_{min} \approx 7.04\tilde{\sigma}_T^{1/1.16}, \tag{18}$$

where $\tilde{\sigma}_T = \sigma_T/\sigma_0$ is the dimensionless tensile strength of the nanotube, with σ_0 as given by Eq. (16). The power law is an excellent fit, as is shown in Fig. 7. The relative error of the power law to the numerically determined values is smaller than 5% over 7 orders of magnitude in $\tilde{L}$.

Equation (18) shows a stronger dependence of the terminal length on tensile strength than the previously predicted scaling of $L_{min} \propto \sigma_T^{1/2}$, which was obtained by neglecting nanotube motion and assuming a constant fluid strain rate along the nanotube.[15,16,18,19,24] In this approximation, the average relative fluid velocity along the nanotube scales with L and the total length over which viscous drag forces are exerted scales with L resulting in an L^2 scaling for the stress exerted on the nanotube. The stronger dependence obtained from our calculations results from the dependence of the maximum fluid strain rate along the nanotube on the length of the nanotube. As is illustrated in Fig. 5, the velocity of a nanotube decreases with increasing length. Longer nanotubes are not dragged along as easily as short ones during bubble collapse and their distance to the center of the bubble remains larger. Because the strain rate of the fluid flow scales with the reciprocal distance cubed, longer nanotubes experience smaller fluid strain rates. This results in a smaller increase in the maximum stress exerted on a nanotube with increasing nanotube length and thus a stronger increase of terminal length with increasing tensile strength.

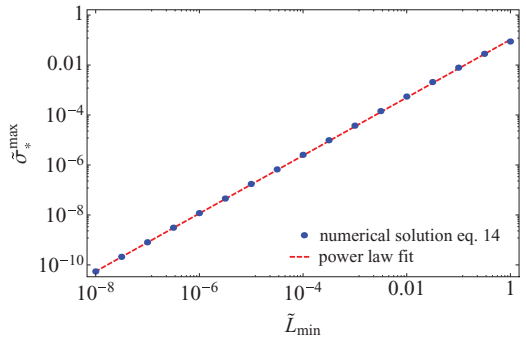

FIG. 7. The dimensionless minimum scission length, $\tilde{L}_{min}$, as a function of the dimensionless tensile strength, $\tilde{\sigma}_T$. The blue dots represent numerical solutions of $\tilde{\sigma}_T = \tilde{\sigma}_*^{max}(\tilde{L}_{min}, y_0 = 1)$. The dashed red curve represents the power law as given by Eq. (18).

When the dimensionless initial distance between a nanotube of length L_{min} and bubble increases beyond $y_0 = 1$, the maximum stress exerted on the nanotube decreases as is evident from Fig. 6. An increase in nanotube length is required if the stress exerted on the nanotube is to exceed the tensile strength of the nanotube. As a result, there is a critical, length-dependent, maximum initial distance from the center of the bubble, $r_{max}(L)$, beyond which scission cannot occur for nanotubes of length less than L.[23] For nanotubes of tensile strength σ_T, scission occurs when $\sigma_*^{max} \geq \sigma_T$. The dimensionless maximum initial distance for which scission of a nanotube of dimensionless tensile strength $\tilde{\sigma}_T$ occurs, y_{max}, can be read off from Fig. 6 by taking the intersection of the horizontal plane of constant $\tilde{\sigma}_T = \tilde{\sigma}_*^{max}$ and the plotted surface. In Fig. 8 the dimensionless critical initial distance,

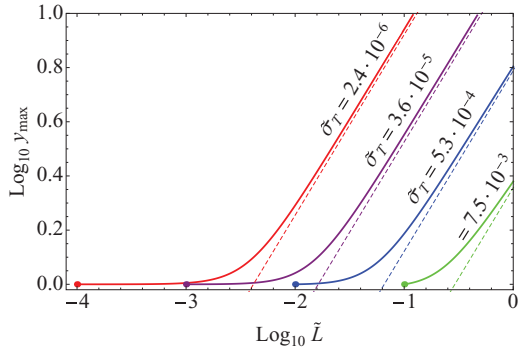

FIG. 8. The dimensionless maximum initial distance, y_{max} for scission to occur as a function of dimensionless nanotube length $\tilde{L}$ for various values of dimensionless tensile strength, $\tilde{\sigma}_T$. Dots show the minimum nanotube length for scission to occur. Dashed lines indicate a power law with exponent 2/3.

y_{max} is shown as a function of dimensionless nanotube length for various values of $\tilde{\sigma}_T$, as obtained by numerically solving $\tilde{\sigma}_*^{max}(\tilde{L}, y_{max}) = \tilde{\sigma}_T$ for y_{max} as a function of $\tilde{L}$. For nanotubes significantly longer than the minimum length a clear power law with slope 2/3 is obtained for all values of $\tilde{\sigma}_T$. This is to be expected because when the nanotube starts out at a sufficiently large distance from the bubble it will not be dragged to region of high fluid strain rate during bubble collapse, and the strain rate of the fluid flow, $\dot{\epsilon}$, as experienced by the nanotube becomes independent of nanotube length and scales with distance as $\dot{\epsilon} \propto r^{-3}$. The stress experienced by the nanotube scales as $\dot{\epsilon} L^2$, so the critical distance must scale as $r_{max} \propto L^{2/3}$.

For very short nanotubes the strain rate must be significantly larger than the strain rate experienced by long nanotubes if scission is to occur. Such an increase in the strain rate occurs for short nanotubes that are close to the surface of the bubble at the point in time when bubble collapse commences. During bubble collapse these short nanotubes are easily dragged along by the fluid flow to distances typically less than $0.1R_{max}$ from the center of the bubble. This results in a significant increase in the experienced strain rate because the strain rate scales with distance as r^{-3}. If we consider a slightly longer nanotube, scission occurs at a lower strain rate of the fluid. However, the maximum strain rate experienced by a nanotube decreases with increasing nanotube length for longer nanotubes are not dragged along as easily. As a result, the allowed increase in the initial distance between nanotube and bubble cannot increase as strongly as it would if the maximum strain rate of the fluid flow experienced by the nanotube is independent of the nanotube length. The critical distance remains close to $y_{max} = 1$ for a large range of nanotube lengths as shown in Fig. 8 and deviates from a power law with slope 2/3 as the maximum strain rate experienced by a nanotube becomes dependent on nanotube length. As we shall shortly see, this has an important consequence, the previously predicted L^2 scission rate[15,23] breaks down near the terminal length, causing the scission kinetics to become non-universal.

Let us now consider how we can derive the scission rate of nanotubes in solution from these findings. If scission occurs when a nanotube of length L starts out at a distance less or equal to $r_{max}(L)$ away from the center of a bubble, then the scission rate, $k(L)$, of a nanotube of length L must be proportional to the probability that a nanotube is found within a distance $r_{max}(L)$ of the center of a bubble at the moment the bubble starts to collapse. Assuming a homogeneous spatial distribution of nanotubes, this probability is proportional to the "scission volume" enclosed between spheres of radius R_{max} and $r_{max}(L)$. We surmise that the scission rate must then obey,

$$k(L) \propto \left(r_{max}(L)^3 - R_{max}^3\right), \tag{19}$$

where the proportionality constant is equal to the number of transiently collapsing bubbles per unit time per unit volume and the scission rate, $k(L)$, gives the fraction of nanotubes of length L that undergo scission per unit time. Note that Pagani *et al.* used similar arguments to derive a scission rate.[23] Let us now focus on the implications for scission kinetics. In Fig. 9,

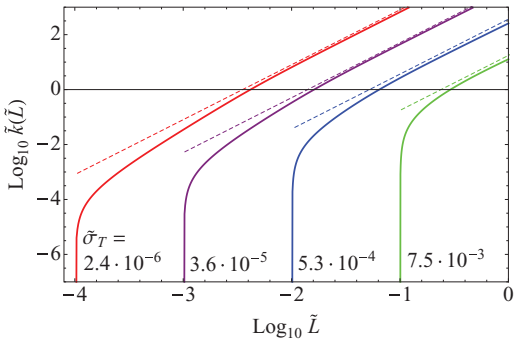

FIG. 9. The dimensionless scission rate, $\tilde{k}(\tilde{L})$ as a function of dimensionless nanotube length $\tilde{L}$ for the same values of dimensionless tensile strength $\tilde{\sigma}_T$ as presented in Fig. 8. The dashed lines correspond to a power law with exponent 2.

the dimensionless scission rate, $\tilde{k}(\tilde{L}) \propto k(\tilde{L})R_{max}^3$, is plotted as a function of dimensionless nanotube length for the same values of $\tilde{\sigma}_T$ as presented in Fig. 8. Here, we have set the dimensionless proportionality constant equal to unity. We can do this, because using its actual value merely shifts the curves upward or downward in the double logarithmic plot.

Fig. 9 shows that the previously derived L^2 scission rate[15,23] breaks down for lengths within an order of magnitude above the minimum scission length while this power law still holds for sufficiently long nanotubes. This is indeed what we expect, because from Fig. 8 we know that nanotube motion only affects the scission mechanics for sufficiently short nanotubes and hence that the L^2 power law, derived by neglecting nanotube motion, must hold for sufficiently long nanotubes. The break down of the universal L^2 power law scission rate for the last three or four scissions before the nanotube reaches a length below the minimum scission length has an important consequence, a non-power law scission rate will yield non-universal scission kinetics. In the discussion, Sec. VI, we will see that this can potentially explain the non-universal scission kinetics as reported in literature.[11,15,19,21]

The scission rate, as shown in Fig. 9, goes to zero at the minimum scission length within our approximation for the minimum scission length is obtained when $y_{max} = 1$, and hence $r_{max}(L_{min}) = R_{max}$. The assumption of a homogeneous nanotube distribution is however tenuous, because nanotubes tend to be concentrated near the surface of the bubble during explosive growth. This happens to be the case, because the nanotubes are slower than the expanding bubble for the same reasons as why the nanotubes cannot keep up with the bubble during bubble collapse. By taking this effect into account, one would arrive at a non-zero scission rate for nanotubes of a length equal to the minimum scission length, L_{min}. However, we choose not to take this into account as it does not qualititatively change the predicted scission rate, while it would require us to model nanotube motion during the explosive growth of the bubble.[48]

Fig. 9 shows that the nanotube properties and the experimental settings determine the length-dependent scission rate through the parameters R_{max} and σ_0 predicted by Eqs. (3) and (16) respectively. Although that for nanotube lengths far larger than L_{min}, we do obtain a universal power

law with exponent 2, the behaviour at lengths close to L_{min} is non-universal. Here scission only occurs because the nanotube is dragged along by the fluid to regions with high strain rate. Transport of the nanotube over a significant length is only possible if the nanotube is short compared to the bubble radius. The smaller $\tilde{L}_{min}$, the larger the length range over which transport is significant and the larger the region over which deviations from the universal power law are observed.

It is clear now that scission occurs only if the nanotube is sufficiently long and if it is sufficiently close to a bubble. To determine the time-evolution of the nanotube length distribution we need to know at which point on the nanotube scission will occur. In Sec. IV we saw that if the nanotube is at a distance of r_{cnt} from the center a bubble, the stress on the nanotube is at a maximum on the point on the nanotube that is at a distance r^* from the center of the bubble, where r^* is given by Eq. (14). It is insightful to define a relative scission position,

$$r^*_{rel}(t) = \frac{r^*(t) - r_{cnt}(t)}{L}, \tag{20}$$

where we note that the position of the nanotube is time-dependent as it is dragged along by the fluid during bubble collapse, and as a consequence of that, the position of maximum stress, r^*, is also time-dependent. The relative scission position is 0.5 if scission occurs at the center of mass of the nanotube, it is 0 for scission at the tip closest to the bubble ($l = -L/2$) and 1 for scission at the far end of the nanotube ($l = L/2$).

To plot the relative scission position, r^*_{rel}, we solve Eq. (17) numerically as a function of $\tilde{L}$ and y_0 to determine the bubble radius, x_{max} at which the stress exerted on the nanotube is at a maximum. Substitution of x_{max} into Eq. (13) produces the corresponding value of r_{cnt}, which, after substitution into Eq. (20) gives the relative scission position. This we plot in Fig. 10 as a function of $\tilde{L}$ and y_0.

Note that, a nanotube with a higher tensile strength will not break for these values of $\tilde{L}$ and y_0, while scission of a nanotube with a lower tensile strength will occur at an earlier moment and thus at a larger value of r_{cnt}. From Eq. (20) follows that the relative scission position, r^*_{rel}, increases with r_{cnt} up to a value of 0.5 for $L/r_{cnt} \to 0$. So, any nanotube with a tensile strength smaller than $\sigma^{max}_*(\tilde{L}, y_0)$ will undergo scission at a point closer to its center than indicated in Fig. 10. As, for a typical sonication experiment,[42] we have $\tilde{L} = 1.5 \times 10^{-3}$ corresponding to a nanotube of a length of approximately 1 μm, scission indeed occurs very close to the center of the nanotube.

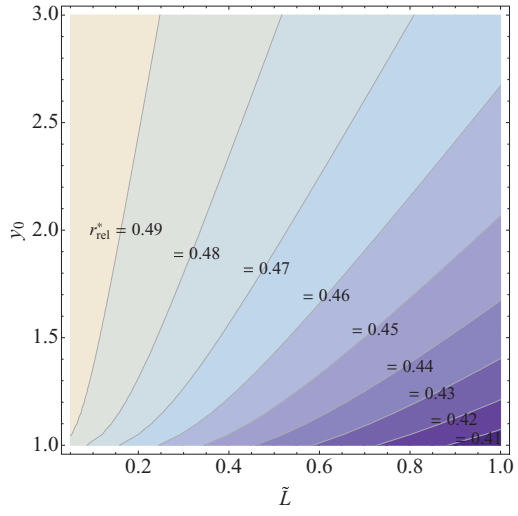

FIG. 10. Contour plot of the relative scission position, r^*_{rel}, as a function of dimensionless nanotube length, $\tilde{L}$, and dimensionless initial distance between nanotube and bubble at the start of the collapse of the bubble, y_0.

VI. DISCUSSION

In Secs. IV and V the mechanics of nanotube scission under tension has been investigated. Key results of the analysis are, (1) an expression for the terminal length, i.e., the length of the shortest nanotube segments that can be reached by means of sonication, (2) the derivation of a non-universal length-dependent scission rate which provides an explanation alternative to the one of Pagani *et al.*[23] for the experimentally observed non-universal scission kinetics, and (3) the determination of the scission position. We showed that the motion of a nanotube during the collapse of a bubble leads to non-universal scission kinetics and affects the scaling of the terminal length with the tensile strength of the nanotube.

Let us first discuss the key assumption underlying our findings, being that nanotubes are oriented radially during bubble collapse. Simulations by Pagani *et al.*[23] indicate that a nanotube relaxes in the initial stages of bubble collapse from an unstable tangential orientation to either a stretched radial conformation through rotation or to a highly bent conformation after buckling. They showed that relaxation by reorientation is favoured by short nanotubes while longer ones bend and buckle. They argued that this is what one would expect, because relaxation by reorientation relies on the breaking of symmetry through rotational diffusion, for a perfectly straight and tangentially oriented nanotube in a perfectly radial fluid flow experiences a net torque of zero. Because rotational diffusion slows down with increasing nanotube length, while the propensity to buckle increases with length, short nanotubes should indeed reorient while longer ones should buckle. This suggests that our model only holds for sufficiently short nanotubes.

We argue that this is not necessarily always the case. Indeed, neglected in the analysis by Pagani *et al.* is, first, the potential presence of defects in the nanotube structure, making them not quite straight and resulting in a break of symmetry. Second, fluctuations in the fluid flow, caused, for example, by other nearby bubbles, can cause a break in the spherical symmetry of the fluid flow. Both of these effects promote the relaxation of longer nanotubes into a stretched radial conformation through a break of symmetry as longer nanotubes arguably contain more defects and are more prone to interact with asymmetries in the fluid flow because they interact with a larger volume of the fluid. Note also that the time scale of both relaxation mechanisms is of the same order of magnitude, as the assumption of Stokesian dynamics ensures that it is the fluid flow that dictates the time scale of any type of motion. Because of this, we argue that short nanotubes

reorient into a radial orientation and scission of these nanotubes is well described by our model, and that for long nanotubes both scission under tension and scission due to overbending can occur. The predominant mechanism is determined by the lack or presence and degree of symmetry breaking during bubble collapse, meaning that an understanding of both scission under tension and scission due to overbending is important for nanotubes of all lengths.

While an analysis of the competition between the two scission mechanisms is beyond the scope of this paper and most likely beyond the scope of analytical theory, it is tempting to speculate about combined breaking scenarios. For instance, even if the nanotube relaxes into a perfectly symmetric and highly bent conformation after buckling, there must still be a competition within the same nanotube between scission due to overbending and scission under tension. The scission under tension mechanism operates on the two highly bent halves of the nanotube, which are aligned nearly radially and thus under high tension. Scission under tension in one of these halves would now result in a segment of a length of a quarter and a segment of three quarters of the length of the nanotube prior to scission. This is of course no more than qualitative reasoning of which we hope to explore the consequences in future work.

We return now to the question how the minimum scission length predicted by our theory and given by Eq. (18) differs from earlier work. First, because we take the previously neglected motion of a nanotube during bubble collapse explicitly into account, we find an exponent of 1/1.16 that differs from the value of 1/2 predicted earlier.[15,16,18,19] Second, we explicitly relate the minimum scission length to the sonication settings and the tensile strength of the nanotube. Interestingly, the minimum scission length scales with the radius of a bubble just prior to it start to collapse as $L_{min} \propto {R_{max}}^{0.14}$. This weak dependence of the minimum scission length on R_{max} suggests that there is indeed a well-defined terminal length, which equals approximately half the minimum scission length, even if there is some spread in the size of the transiently collapsing bubbles.

It is however doubtful whether the terminal length is observed in experiments.[19] Experiments show a power law relation between the average length of nanotubes and the time for which they have been sonicated,[11,15,19,21] suggesting that the terminal length has not been reached in these experiments. Indeed, when a significant number of the nanotubes have a length close to the minimum scission length, one would expect the number of nanotubes with a length above the minimum scission length to decrease exponentially over time. This is because scission of these nanotubes is essentially a first-order "reaction" in which the nanotubes go from being able to undergo scission to being unable to undergo scission, for after scission the resulting segments have a length below the minimum scission length. Intuitively one would expect the power law relating average length to time to break down if the number of the nanotubes available to undergo scission starts to decrease exponentially. This discrepancy is possibly resolved by our work, which shows the scission rate to decrease by several orders of magnitude when the length of the nanotubes approaches the minimum scission length, see Fig. 9. This suggests that experimental time scales might indeed be too short to observe the terminal length.

The experimentally observed power law relation between the average nanotube length and sonication time[11,15,19,21] has been reproduced by a simple kinetic model for a power law scission rate.[19,23] In this kinetic model the length-dependent scission rate is assumed to obey a simple power law, $k(L) \propto L^{1/\alpha}$, meaning that there is no terminal length below which scission stops in this kinetic model. By treating the scission of nanotubes as a first-order reaction, and by assuming an initially monodisperse length-distribution and finally by imposing conservation of carbon nanotube mass, one can derive that the average length must scale with sonication time as $\langle L \rangle \propto t^{-\alpha}$. This, in light of our discussion so far, is a remarkable result. By assuming that there is no terminal length the experimentally observed power law decrease of the average length over time is reproduced, which, again, suggests that the terminal length is not reached on experimental time scales.

We can use the same simple kinetic model to compare the results of our model with experimental results. Let us first consider the situation where all nanotubes have a length well above the minimum scission length. Here, our model predicts that the scission rate is a power law with exponent $\alpha^{-1} = 2$ and the kinetic model predicts the power law relating average length and sonication time to have an exponent of $\alpha = 0.5$, in agreement with some experimental results.[15] However, an experimentally determined value of $\alpha = 0.22$ has also been reported,[19] which corresponds to a slow down of the scission kinetics as compared to the situation where $\alpha = 0.5$.

This is potentially explained by our model, which predicts the scission kinetics to slow down significantly near the minimum scission length, as compared to the situation where the scission rate is an L^2 power law, for here our model predicts the scission rate to deviate from a pure power law with exponent $\alpha^{-1} = 2$. This deviation from a power law is significant in terms of scission kinetics. For a power law, the scission kinetics must be identical at all length scales while this is not necessarily true for a non-power law scission rate. This suggests that the scission kinetics depends on how many of the nanotubes are sufficiently close to the terminal length to have their scission governed by the non-power law region of the scission rate as predicted by our model. Interestingly, our model predicts that deviations from a 0.5 power law occur when close to the terminal length, this is in contradiction with the work by Pagani *et al.*[23] who predict that the scission rate of long nanotube that buckle and break deviates from a 0.5 power law and follows a 0.25 power law. Unfortunately, the current kinetic model is too simple to come to a sensible comparison of our model with experimental results. The kinetic model only allows for the analysis of a simple power law scission rate and does not take the existence of a terminal length into account and hence is not suited to the analysis of the results of our model. Although our model certainly predicts the scission kinetics to be slower than a 0.5 power law when close to the terminal length, we believe that a more thorough study of the scission kinetics, using a more advanced kinetic model, is required to see if our model can reproduce the

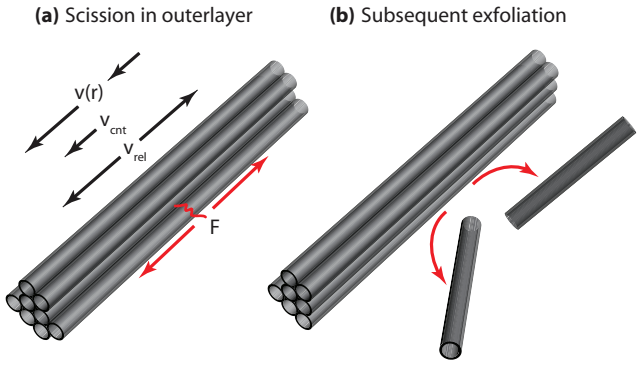

FIG. 11. The exfoliation of a nanotube rope by scission of individual nanotubes in the outer layer. Nanotube ropes will be dragged along by the fluid flow following the transient collapse of a bubble just like a single nanotube. Strong gradient in the fluid velocity results in a large stress exerted on the nanotubes on the outer layer of the rope, possibly causing scission of these nanotubes. After scission the two resulting segments will be "pulled of" the bundle if the drag force exerted by the fluid flow exceeds the binding force between the nanotube segment and the bundle.

experimentally observed exponent of 0.22. This, we intend to pursue in the near future.

We end this paper with a discussion of the connection between sonication and exfoliation, where we recall that scission is an unwanted by-effect of sonication. Any attempt to optimise the sonication process requires an understanding of both the mechanics and kinetics of exfoliation and scission. The exfoliation of single-wall carbon nanotubes bundles has been attributed to the diffusion of surfactant molecules into nanotube bundles after cracks are formed in these bundles by means of sonication. When a surfactant layer has formed between a nanotube and the bundle it is part of, this nanotube is separated from the bundle.[6,8] Here, we would like to propose a different mechanism. If nanotube bundles orient into a radial orientation during bubble collapse, just as individual nanotubes do, scission of a nanotube in the outer layer of the bundle can occur when the stress exerted by the fluid flow exceeds the tensile strength of the nanotube. After scission has occurred, the fluid exerts large drag forces on each of the resulting nanotube halves. If these drag forces exceed the binding force between bundle and nanotube segment, the nanotube segments slide off the bundle and are separated from the bundle. In this scenario exfoliation relies on nanotube scission as is illustrated schematically in Fig. 11. If this process is indeed responsible for the exfoliation of nanotube bundles, then the sonication process can be optimised. The sonication power should be just sufficient to cause scission of nanotube in the outer layer of the bundle, while it should be insufficient to cause the scission of the resulting nanotube segments that have a length approximately equal to half the length of the nanotubes in the bundle. Here, a more thorough analysis is required that we will pursue in the near future.

In conclusion, we have shown that scission of nanotubes under tension during bubble collapse does not result in universal scission kinetics. This can potentially explain the variety in the experimentally observed scission kinetics and is in contrast with previous work on scission under tension in which scission under tension was thought to result in universal kinetics. Given the length-dependent scission rate, Eq. (19), the lengths of the segments resulting from scission, Eq. (20), and the terminal scission length, Eq. (18), the scission kinetics, and the time-evolution of the length distribution are fully determined, allowing, in principle for controlled manipulation of the length distribution. Finally, if exfoliation is indeed scission-mediated, knowledge of both scission and exfoliation kinetics will allow for optimisation of the sonication process.

ACKNOWLEDGMENTS

I would like to acknowledge Professor Paul van der Schoot for discussions and for the critical reading of this manuscript.

[1]C. Koning, N. Grossiord, and M. C. Hermant, *Polymer Carbon Nanotube Composites: The Polymer Latex Concept* (Pan Stanford Publishing, 2012).
[2]M. S. Dresselhaus, G. Dresselhaus, and P. Avouris, *Carbon Nanotubes: Synthesis, Structure, Properties and Applications* (Springer, 2001).
[3]P. J. F. Harris, *Carbon Nanotube Science: Synthesis, Properties and Applications* (Cambridge University Press, 2009).
[4]Z. Wu, Z. Chen, X. Du, J. M. Logan, J. Sippel, M. Nikolou, K. Kamaras, J. R. Reynolds, D. B. Tanner, A. F. Hebard, and A. G. Rinzler, Science **305**, 1273 (2004).
[5]A. V. Kyrylyuk, M. C. Hermant, T. Schilling, B. Klumperman, C. Koning, and P. van der Schoot, Nat. Nanotechnol. **6**, 364 (2011).
[6]R. Bandyopadhyaya, E. Nativ-Roth, O. Regev, and R. Yerushalmi-Rozen, Nano Lett. **2**, 25 (2002).
[7]M. F. Islam, E. Rojas, D. M. Bergey, A. T. Johnson, and A. G. Yodh, Nano Lett. **3**, 269 (2003).
[8]M. S. Strano, V. C. Moore, M. K. Miller, M. J. Allen, E. H. Haroz, C. Kittrell, R. H. Hauge, and R. Smalley, J. Nanosci. Nanotechnol. **3**, 81 (2003).
[9]N. Grossiord, O. Regev, J. Loos, J. Meuldijk, and C. Koning, Anal. Chem. **77**, 5135 (2005).
[10]J. Yu, N. Grossiord, C. Koning, and J. Loos, Carbon **45**, 618 (2007).
[11]T. Liu, S. Luo, Z. Xiao, C. Zhang, and B. Wang, J. Phys. Chem. C **112**, 19193 (2008).
[12]T. Liu, Z. Xiao, and B. Wang, Carbon **47**, 3529 (2009).
[13]R. H. J. Otten and P. van der Schoot, J. Chem. Phys. **134**, 094902 (2011).
[14]D. A. Heller, R. M. Mayrhofer, S. Baik, Y. V. Grinkova, M. L. Usrey, and M. S. Strano, J. Am. Chem. Soc. **126**, 14567 (2004).
[15]F. Hennrich, R. Krupke, K. Arnold, J. Rojas Stutz, S. Lebedkin, T. Koch, T. Schimmel, and M. Kappes, J. Phys. Chem. B **111**, 1932 (2007).
[16]S. Ahir, Y. Huang, and E. Terentjev, Polymer **49**, 3841 (2008).
[17]H. J. Park, M. Park, J. Y. Chang, and H. Lee, Nanotechnology **19**, 335702 (2008).
[18]Y. Y. Huang, T. P. J. Knowles, and E. M. Terentjev, Adv. Mater. **21**, 3945 (2009).
[19]A. Lucas, C. Zakri, M. Maugey, M. Pasquali, P. van der Schoot, and P. Poulin, J. Phys. Chem. C **113**, 20599 (2009).
[20]Q. Cheng, S. Debnath, E. Gregan, and H. J. Byrne, J. Phys. Chem. C **114**, 8821 (2010).
[21]A. J. Blanch, C. E. Lenehan, and J. S. Quinton, Carbon **49**, 5213 (2011).
[22]H. B. Chew, M. W. Moon, K. R. Lee, and K. S. Kim, Proc. R. Soc. London, Ser. A **467**, 1270 (2011).
[23]G. Pagani, M. J. Green, P. Poulin, and M. Pasquali, Proc. Natl. Acad. of Sci. U.S.A. **109**, 11599 (2012).
[24]Y. Y. Huang and E. M. Terentjev, Polymers **4**, 275 (2012).
[25]M. Ashokkumar, J. Lee, S. Kentish, and F. Grieser, Ultrason. Sonochem. **14**, 470 (2007).
[26]T. G. Leighton, *The Acoustic Bubble* (Academic Press, 1994).
[27]E. A. Neppiras, Ultrasonics **22**, 25 (1984).
[28]A. Prosperetti, Ultrasonics **22**, 69 (1984).
[29]A. Prosperetti, Ultrasonics **22**, 115 (1984).
[30]R. E. Apfel, Ultrasonics **22**, 167 (1984).
[31]L. A. Crum, Ultrasonics **22**, 215 (1984).
[32]R. E. Apfel, J. Acoust. Soc. Am. **69**, 1624 (1981).

[33]M. W. Kuijpers, P. D. Iedema, M. F. Kemmere, and J. T. Keurentjes, Polymer **45**, 6461 (2004).
[34]A. Akyuz, H. Catalgil-Giz, and A. T. Giz, Macromol. Chem. Phys. **209**, 801 (2008).
[35]H. I. Elsner and E. B. Lindblad, DNA **8**, 697 (1989).
[36]G. Guerin, H. Wang, I. Manners, and M. A. Winnik, J. Am. Chem. Soc. **130**, 14763 (2008).
[37]M.-F. Yu, O. Lourie, M. J. Dyer, K. Moloni, T. F. Kelly, and R. S. Ruoff, Science **287**, 637 (2000).
[38]M.-F. Yu, B. S. Files, S. Arepalli, and R. S. Ruoff, Phys. Rev. Lett. **84**, 5552 (2000).
[39]J. W. Rayleigh, Philos. Mag. **34**, 94 (1917).
[40]J. B. Keller and S. I. Rubinow, J. Fluid Mech. **75**, 705 (1976).
[41]J. Pittman and N. Kasiri, Int. J. Multiphase Flow **18**, 1077 (1992).
[42]We define a typical sonication experiment as sonication at 40 W and a frequency of 20 kHz where the sonicator horn has a diameter of 15 mm. Sonication takes place in water under ambient conditions. In the typical sonication experiment single wall nanotubes with a tensile strength of 30 GPa, a diameter of 1.3 nm and a wall thickness of 0.3 nm are sonicated.
[43]Calculations by Professor Paul van der Schoot.
[44]R. Duggal and M. Pasquali, Phys. Rev. Lett. **96**, 246104 (2006).
[45]N. Fakhri, D. A. Tsyboulski, L. Cognet, R. B. Weisman, and M. Pasquali, Proc. Natl. Acad. Sci. U.S.A. **106**, 14219 (2009).
[46]The Reynolds number is defined as $Re = \rho v L/\mu$, where ρ is the mass density of the liquid, v the mean relative velocity of the fluid relative to the object, L is the characteristic length of the object, and μ is the dynamic viscosity of the fluid.
[47]If we assume a linear flow profile and equate the stress on the nanotube to the tensile strength, σ_T of the nanotube we find $\sigma_T = \pi\mu\dot{\epsilon}L^2/2A$. The maximum relative fluid velocity occurs at the nanotube tips and is given by $v_{max} = \dot{\epsilon}L/2 = \sigma_T A/\pi\mu L$. Using this as the characteristic velocity and the nanotube diameter as the characteristic length-scale we find a maximum Reynolds number of the order of 1 for the fluid flow around the nanotube.
[48]We checked this by modelling nanotube motion during explosive growth of the bubble by calculating the motion of a nanotube with an orientation tangential to the bubble surface. The result allows us to calculate the distance away from the center of the bubble at the start of explosive growth, d_i, for which the nanotube will be at a distance r_{max} from the center of the bubble at the end of explosive growth. We calculate the scission rate by assuming it is proportional to d_i^3. The resulting scission rate has a non-zero value at the minimum scission length, L_{min}, but is qualitatively identical to the scission rate as derived by neglecting nanotube motion during explosive growth of the bubble.